AD-753 389

FLOW FIELD ON THE LEE SIDE OF A DELTA WING

Robert Gene Christophel

Air Force Institute of Technology
Wright-Patterson Air Force Base, Ohio

December 1971

UNITED STATES AIR FORCE

AIR UNIVERSITY

AIR FORCE INSTITUTE OF TECHNOLOGY

Wright-Patterson Air Force Base, Ohio

FLOW FIELD ON THE LEE SIDE OF A DELTA WING

THESIS

GAM/AE/72-6 Robert G. Christophel
2Lt USAF

Ia

Unclassified
Security Classification

DOCUMENT CONTROL DATA - R & D

(Security classification of title, body of abstract and indexing annotation must be entered when the overall report is classified)

ORIGINATING ACTIVITY (Corporate author)
Air Force Institute of Technology (AFIT-EN)
Wright-Patterson AFB, Ohio 45433

2a. REPORT SECURITY CLASSIFICATION
Unclassified

2b. GROUP

3. REPORT TITLE
Flow Field on the Lee Side of a Delta Wing

4. DESCRIPTIVE NOTES (Type of report and inclusive dates)
AFIT Thesis

5. AUTHOR(S) (First name, middle initial, last name)
Robert G. Christophel
2Lt USAF

6. REPORT DATE	7a. TOTAL NO. OF PAGES	7b. NO. OF REFS
December 1971	~~54~~ 58	13

8a. CONTRACT OR GRANT NO.	9a. ORIGINATOR'S REPORT NUMBER(S)
b. PROJECT NO.	GAM/AE/72-6
c.	9b. OTHER REPORT NO(S) (Any other numbers that may be assigned this report)
d.	

10. DISTRIBUTION STATEMENT
Approved for public release; distribution unlimited.

Approved for public release; IAW AFR 190-17
Jerry C. Hix, Captain, USAF
Director of Information

12. SPONSORING MILITARY ACTIVITY
ARL/LH

13. ABSTRACT

A procedure is developed which utilizes the method of characteristics to solve a portion of the flow field on the lee side of a flat plate delta wing with supersonic leading edges at angle of attack but at zero yaw. The procedure requires input conditions of a free stream Mach number M_∞, an angle of attack α, and a sweep angle χ.

The procedure is applied to the following three sets of input conditions: 1) $M_\infty=2.96$, $\alpha=14.2^\circ$, $\chi=45.0^\circ$; 2) $M_\infty=4.0$, $\alpha=5.0^\circ$, $\chi=60.0^\circ$; 3) $M_\infty=3.0$, $\alpha=12.0^\circ$, $\chi=45.0^\circ$. The resulting data is then compared to published experimental and analytical data for the same set of input conditions.

The comparisons indicate that the procedure developed here may be useful in predicting the flow field in the pseudo-elliptic region and the position of the internal shock wave on the lee side of the wing.

DD FORM 1 NOV 68 1473

I f

Unclassified
Security Classification

Unclassified
Security Classification

KEY WORDS	LINK A		LINK B		LINK C	
	ROLE	WT	ROLE	WT	ROLE	WT
Method of Characteristics						
Delta Wing						
Conical Flow						
Lee Side Flow Field						
Supersonic Flow						
Hypersonic Flow						
Supersonic Leading Edges						
Three Dimensional Flow						
Steady Flow						
Angle of Attack						
Numerical Analysis						

IC

Unclassified
Security Classification

FLOW FIELD ON THE LEE SIDE OF A DELTA WING

THESIS

Presented to the Faculty of the School of Engineering
of the Air Force Institute of Technology
Air University
in Partial Fulfillment of the
Requirements for the Degree of
Master of Science
by

Robert G. Christophel, B.S.
2Lt USAF

Graduate Aerospace-Mechanical Engineering

December 1971

I d

Preface

This thesis represents the results of an effort to write a computer program for the CDC 6600 computer to solve for a portion of the flow field on the lee side of a delta wing with supersonic leading edges. The problem was first proposed by Dr. William L. Hankey of the Aerospace Research Laboratory and Captain John V. Kitowski who is on the faculty of the Air Force Institute of Technology. Captain Kitowski also acted as thesis advisor and I would like to express my sincere gratitude for his many hours of advice and encouragement during the period of this study.

I would like to express my deep appreciation and gratitude to my wife, Cherolette, for her understanding, patience, and encouragement during my entire AFIT tour.

Also, I would like to thank Mrs. Anne E. Posner for the typing of this paper.

Robert G. Christophel

Contents

List of Figures

List of Symbols

A	Square of the dimensionless speed of sound $(\frac{c}{V_\infty})^2$
M	Local Mach number
M_c	Local crossflow Mach number
P	Pressure
S	Entropy
T	Temperature
$\overline{U}$	Total velocity vector
V	Magnitude of total velocity
X, Y, Z	Cartesian coordinate system
a_1, a_2, a_3	Defined by equations (34), (35), and (36)
b	Defined by equation (15)
b_1, b_2, b_3, b_4	Defined by equations (42), (43), (44) and (45)
c	Local speed of sound
$\hat{n}$	Unit vector normal to streamline
s	Dimensionless entropy
u, v, w	Dimension velocity components in the X, Y, and Z directions respectively (actual velocity components divided by V_∞)
x, y, z	Coordinates in the Cartesian system
α	Angle of attack
α_1	Angle between the component of free stream velocity normal to the leading edge and the wing surface

β	Angle between the free stream velocity vector and the leading edge
γ	Ratic of specific heats
δ	Flow deflection angle
η	Dimensionless coordinate $(\frac{y}{x})$
θ	Term in the Prandtl-Meyer function
μ	Mach angle
ξ	Dimensionless coordinate $(\frac{z}{x})$
ρ	Density
ϕ	Angle between a Prandtl-Meyer expansion ray and the wing surface
χ	Sweep angle
ψ	Term in the Prandtl-Meyer function
$\bar{\omega}$	Vorticity

Subscripts

∞	Free stream condition
n	Normal to leading edge
p	Pitot pressure
t	Parallel to leading edge

FLOW FIELD ON THE LEE SIDE OF A DELTA WING

I. Introduction

This study is concerned with the flow field on the lee side of a flat plate delta wing with supersonic leading edges. As shown in Fig.1, the wing is placed at an angle of attack α and at zero yaw.

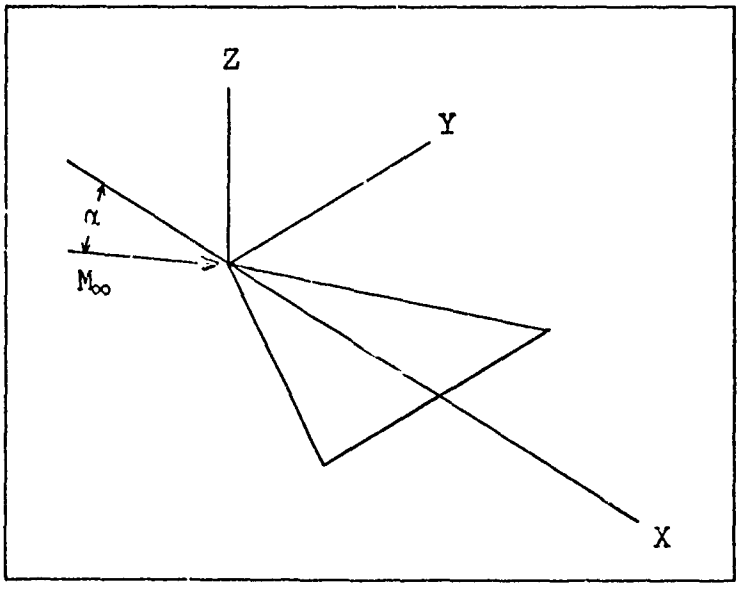

Figure 1. Coordinate System

The vertex of the wing is placed at the origin of a rectangular Cartesian coordinate system. The flow medium is assumed to be an inviscid, non-heatconducting, nonreacting,

ideal gas. The free stream is assumed to be uniform and steady.

The general flow pattern on the expansion side of the wing is symmetrical with respect to the XZ plane and a sketch of the flow pattern on the lee side is given in Fig. 2.

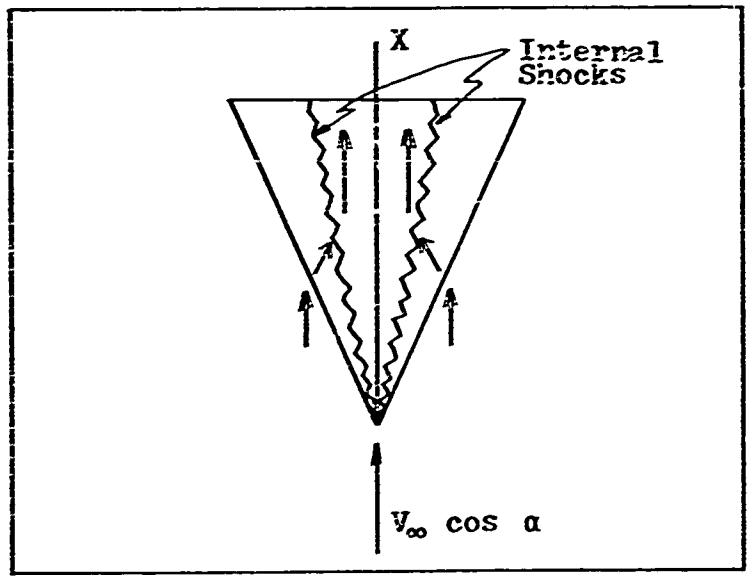

Figure 2. Flow Pattern on Surface

As the free stream flows over the leading edge, the component of velocity parallel to the leading edge is not altered but the component normal to the leading edge must expand to become parallel to the surface of the wing. This results in the total velocity vector on the surface of the wing immediately downstream of the leading edge having a component normal to the root chord. However, because of the symmetry, the total velocity vector at the root chord must be parallel to the root chord. Therefore, as indicated

in Fig. 2, the total velocity vector on the surface of the wing must change direction and this condition is brought about by the formation of an internal shock wave which is attached to the upper surface.

The flow field for a flat plate delta wing with supersonic leading edges is conical as conceived by Busemann (Ref 5) and, as such, the flow field in any plane normal to the root chord has a similar solution. Thus, the entire

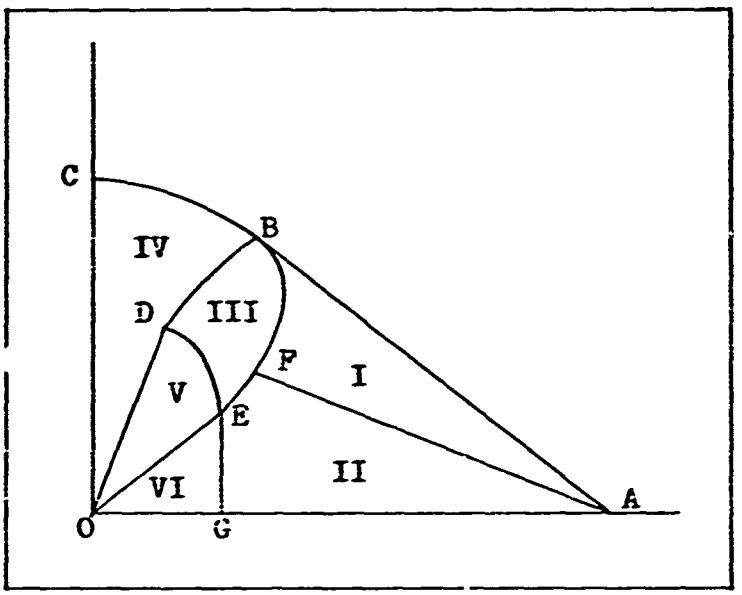

Figure 3. Crossflow Plane

lee side flow field may be represented by any arbitrarily selected plane which is normal to the root chord. This plane is called the "crossflow" plane and a qualitative sketch of the right half of the plane is shown in Fig. 3.

The crossflow plane may be separated into six regions with distinct characteristics as indicated in Fig. 3. The governing equations in regions I, II, and III are

hyperbolic. The governing equations in regions IV, V, and VI are elliptic. Line BD represents a crossflow sonic line along which the governing equations are parabolic. Line DEG is an internal shock wave. The segment GE is planar but the segment DE is curved. Line AB represents the first ray of a Prandtl-Meyer expansion fan. Line BFE is the reflection of this expansion ray from the surface of the cone of excitation BC which emanates from the vertex of the wing. Line AF represents the last ray of the Prandtl-Meyer expansion fan. Lines OD and OE are crossflow streamlines separating the rotational flow in region V from the irrotational flow in regions IV and VI. Line OGA is the wing surface and line OC represents the plane of symmetry.

Among the analytical solutions to this flow field are those presented by Maslen (Ref 13), Babayev (Ref 1), Beeman and Powers (Ref 3), and Kutler and Lomax (Ref 11). Powell (Ref 8) presented an analytical solution along with experimental data for the flow field. Bannink, Nebbling, and Reyn (Ref 2) conducted an experimental investigation of the flow field as did Cross and Hankey (Ref 7). A compilation of papers treating the mathematical theory of conical flows is presented in the work of Bulekh and Reyn (Ref 4).

In Maslen's treatment of the problem, it was assumed there were no internal shock waves in the flow field and a solution was obtained by using Prandtl-Meyer relations in regions I and II and a relaxation method in the remainder of the flow field. Powell experimentally determined the existence of an internal shock wave and then assumed the

shock wave was planar and used an approximate method to locate the shock wave and solve for the flow adjacent to the wing surface. The solution presented by Babayev also included an internal planar shock wave but the flow field in regions III, IV, V, and VI was determined from irrotational potential flow theory using the method of successive approximations. Beemann and Powers assumed the existence of an internal shock wave and attempted to solve the problem by using a modified method of characteristics scheme. However, as a result of difficulties with the internal shock calculations, only shock-free results were reported. In the experimental work of Bannink, Nebbeling, and Reyn, the existence of an internal shock wave was reconfirmed but the shock wave was found to be curved.

In all of the analytical studies cited above it is assumed that flow in region III is dependent on the flow in regions IV, V, and VI. The approach taken in this study is to solve the flow field in region III by reducing the inviscid flow governing equations using conical flow conditions and then applying the method of characteristics to the resulting hyperbolic equations. The results of this study may then be applied to the solution of the flow field in the elliptic region.

II. The Development of Equations

The crossflow plane may be taken as any YZ plane that intersects the positive X-axis. This plane is nondimensionalized by using the dimensionless coordinates and ,

where
$$\xi = \frac{Z}{X} \tag{1}$$

and
$$\eta = \frac{Y}{X} \tag{2}$$

The governing equations are transformed to the crossflow plane by means of these dimensionless coordinates.

Line BC - Cone of Excitation

The cone of excitation which is generated by the apex of the delta wing is given by,

$$\sqrt{Y^2 + (-X \sin\alpha + Z \cos\alpha)^2} - (X \cos\alpha + Z \sin\alpha) \tan\mu = 0 \tag{3}$$

In terms of ξ and η this becomes

$$\sqrt{\eta^2 + (\xi\cos\alpha - \sin\alpha)^2} - (\cos\alpha + \xi\sin\alpha) \tan\mu = 0 \tag{4}$$

or, since, $\tan\mu = (M_\infty^2 - 1)^{-\frac{1}{2}}$

$$\left(1 - \frac{1}{M_\infty^2}\right)\left(1 + \xi^2 + \eta^2\right) = \left(\cos\alpha + \xi \sin\alpha\right)^2 \qquad (5)$$

Region I - Prandtl-Meyer Expansion Fan

The development of the equations in this section follows closely that of Babayev.

From the classical Prandtl-Meyer relationship, as given in Liepmann and Roshko (Ref 12:98-100), the local flow deflection δ in a plane normal to the leading edge is given by

$$\delta = \sqrt{\frac{\gamma+1}{\gamma-1}}\tan^{-1}\sqrt{\frac{\gamma-1}{\gamma+1}\left(M_n^2-1\right)} - \tan^{-1}\sqrt{M_n^2-1}$$

$$-\sqrt{\frac{\gamma+1}{\gamma-1}}\tan^{-1}\sqrt{\frac{\gamma-1}{\gamma+1}\left(M_{n_\infty}^2-1\right)} + \tan^{-1}\sqrt{M_{n_\infty}^2-1} \qquad (6)$$

or, by letting

$$\theta = \sqrt{\frac{\gamma+1}{\gamma-1}}\tan^{-1}\sqrt{\frac{\gamma-1}{\gamma+1}\left(M_n^2-1\right)} \qquad (7)$$

and

$$\psi = \tan^{-1}\sqrt{M_n^2-1} \qquad (8)$$

equation (6) reduces to

$$\delta = \theta - \tan^{-1}\left(\sqrt{\frac{\gamma+1}{\gamma-1}}\tan\sqrt{\frac{\gamma-1}{\gamma+1}}\theta\right) - \theta_\infty + \psi_\infty \qquad (9)$$

The dimensionless velocity components in region I are given as functions of δ by

$$u = b \cos(\alpha_1 - \delta) \cos\lambda + \cos\beta \sin\lambda \tag{10}$$

$$v = -b \cos(\alpha_1 - \delta) \sin\lambda + \cos\beta \cos\lambda \tag{11}$$

$$w = b \sin(\alpha_1 - \delta) \tag{12}$$

where
$$\alpha_1 = \tan^{-1}\left(\frac{\tan\alpha}{\cos\lambda}\right) \tag{13}$$

$$\beta = \cos^{-1}(\cos\alpha \sin\lambda) \tag{14}$$

and
$$b^2 = \left[\frac{2}{\gamma+1}\frac{1}{M_\infty^2} + \frac{\gamma-1}{\gamma+1}(1 - \cos^2\beta)\right]$$
$$\left[1 + \frac{2}{\gamma-1}\sin^2\sqrt{\frac{\gamma-1}{\gamma+1}}\theta\right] \tag{15}$$

Equations (10), (11), and (12) are developed in detail in Appendix A.

In the plane normal to the leading edge the angle between a Prandtl-Meyer expansion ray and the surface of the wing is given by

$$\sigma = \theta_\infty - \nu_\infty + \frac{\pi}{2} - \theta + \alpha_1 \tag{16}$$

By noting that
$$\tan\sigma = \frac{\xi}{\cos\lambda - \eta\sin\lambda} \tag{17}$$

the slope of the expansion ray in the ξ, η plane may be obtained by substituting equation (17) into equation (16) and differentiating. This results in

$$\left(\frac{d\xi}{d\eta}\right)_{\text{exp ray}} = -\sin\lambda \tan\left(\theta_\infty - \nu_\infty + \frac{\pi}{2} + \alpha_1 - \theta\right) \quad (18)$$

setting $\xi = 0$ in equation (17) gives the η-value of the intersection of all expansion rays with the η-axis as

$$\eta_{max} = \cot\lambda \quad (19)$$

Equations (10), (11), (12), (18), and (19) completely determine the dimensionless velocity distribution throughout region I. Other flow properties may be determined from the isentropic relationships.

Region II - Fully Expanded Area

The flow properties in region II are determined completely by the values along the last expansion ray. This is a result of the fact that the flow properties are constant throughout the region.

Setting $\delta = \alpha_1$ in equation (9) results in the expression for the value of θ along the last expansion ray as

$$\theta_{cr} = \alpha_1 + \theta_\infty - \nu_\infty + \tan^{-1}\left(\sqrt{\frac{\gamma+1}{\gamma-1}}\tan\sqrt{\frac{\gamma-1}{\gamma+1}}\theta_{cr}\right) \quad (20)$$

Point B - Intersection of Cone of Excitation and First Expansion Ray

The cone of excitation intersects the first expansion ray at the point where the slopes of these lines are equal. From equation (13) the slope of the first expansion ray is

$$\left(\frac{d\xi}{d\eta}\right)_{\text{exp ray 1}} = -\frac{\sin\lambda}{\tan(\psi_\infty - \alpha_1)} \tag{21}$$

and differentiation of equation (5) results in

$$\left(\frac{d\xi}{d\eta}\right)_{\text{cone}} = -\frac{(1-\frac{1}{M_\infty^2})\eta}{(1-\frac{1}{M_\infty^2})\xi - \sin\alpha(\cos\alpha + \zeta\sin\alpha)} \tag{22}$$

Equating equations (21) and (22) results in the ξ intersection value ξ_{int} of

$$\xi_{int} = \frac{(1-\frac{1}{M_\infty^2})\left[\frac{\tan(\psi_\infty - \alpha_1)}{\sin\lambda\tan\lambda}\right] + \sin\alpha\cos\alpha}{(1-\frac{1}{M_\infty^2})\left\{1 + \left[\frac{\tan(\psi_\infty - \alpha_1)}{\sin\lambda}\right]^2\right\} - \sin^2\alpha} \tag{23}$$

The intersection value η_{int} may be obtained from equation (5).

Region III - Pseudo-Elliptic Area

The development of the equations for region III closely follows that of Chaing and Wagner (Ref 6) who present a detailed derivation of the governing equations for non-isentropic flow.

The continuity, momentum, and energy equations can be written in vector form as

$$\nabla \cdot (\rho \bar{U}) = 0 \tag{24}$$

$$\bar{\omega} \times \bar{U} = \bar{T} \nabla S \tag{25}$$

$$\bar{U} \cdot \nabla S = 0 \tag{26}$$

Using the conical flow conditions, the equations may be rewritten for the ξ, η plane as

$$2A \left(\eta \frac{\partial u}{\partial \eta} + \xi \frac{\partial u}{\partial \xi} - \frac{\partial v}{\partial \eta} - \frac{\partial w}{\partial \xi} \right)$$

$$- (\eta u - v) \left[\frac{\partial}{\partial \eta} (u^2 + v^2 + w^2) \right]$$

$$- (\xi u - w) \left[\frac{\partial}{\partial \xi} (u^2 + v^2 + w^2) \right] = 0 \tag{27}$$

$$v \left(\eta \frac{\partial v}{\partial \eta} + \xi \frac{\partial v}{\partial \xi} + \frac{\partial u}{\partial \eta} \right) + w \left(\eta \frac{\partial w}{\partial \eta} + \xi \frac{\partial w}{\partial \xi} + \frac{\partial u}{\partial \xi} \right)$$

$$= - A \left(\eta \frac{\partial s}{\partial \eta} + \xi \frac{\partial s}{\partial \xi} \right) \tag{28}$$

$$u\left(\eta\frac{\partial v}{\partial \eta}+\xi\frac{\partial v}{\partial \xi}+\frac{\partial u}{\partial \eta}\right)+w\left(\frac{\partial w}{\partial \eta}-\frac{\partial v}{\partial \xi}\right)=-A\frac{\partial s}{\partial \eta} \tag{29}$$

$$u\left(\eta\frac{\partial w}{\partial \eta}+\xi\frac{\partial w}{\partial \xi}+\frac{\partial u}{\partial \xi}\right)+v\left(\frac{\partial v}{\partial \xi}-\frac{\partial w}{\partial \eta}\right)=-A\frac{\partial s}{\partial \xi} \tag{30}$$

$$(\eta u-v)\frac{\partial s}{\partial \eta}+(\xi u-w)\frac{\partial s}{\partial \xi}=0 \tag{31}$$

where A is given by

$$A=\frac{1}{M_\infty^2}+\frac{\gamma-1}{2}\left(1-u^2-v^2-w^2\right) \tag{32}$$

Equation (28) is a linear combination of equations (29), (30), and (31) and it may then be discarded. By manipulating equations (27), (29), (30), and (31) and using the definition of a total derivative the following set of equations may be written in matrix form as

$$\begin{vmatrix} a_1 & a_2 & a_3 & a_1 \\ 1 & 0 & 0 & -1 \\ d\xi & d\eta & 0 & 0 \\ 0 & 0 & d\xi & d\eta \end{vmatrix} \begin{vmatrix} \left(\frac{\partial v}{\partial \xi}\right) \\ \left(\frac{\partial v}{\partial \eta}\right) \\ \left(\frac{\partial w}{\partial \xi}\right) \\ \left(\frac{\partial w}{\partial \eta}\right) \end{vmatrix} = \begin{vmatrix} G \\ Q \\ dv \\ dw \end{vmatrix} \tag{33}$$

where $$a_1 = A\xi\eta - (\eta u - v)(\xi u - w) \tag{34}$$

$$a_2 = A(1+\eta^2) - (\eta u - v)^2 \tag{35}$$

$$a_3 = A(1+\xi^2) - (\xi u - w)^2 \tag{36}$$

$$Q = \frac{A\,ds + u(du + \eta dv + \xi dw)}{(\eta u - v)\,d\xi - (\xi u - w)\,d\eta} \tag{37}$$

and $$G = \frac{A(\xi u - \eta w)(du + \eta dv + \xi dw)}{(\eta u - v)\,d\xi - (\xi u - w)\,d\eta} \tag{38}$$

Setting the coefficient matrix of equation (33) equal to zero gives the slope of the characteristics as

$$\left(\frac{d\xi}{d\eta}\right)_{\pm c} = \frac{a_1 \pm \sqrt{a_1^2 - a_2 a_3}}{a_2} \tag{39}$$

The compatibility equations for these characteristics are obtained by setting the determinant

$$\begin{vmatrix} a_1 & a_2 & a_3 & G \\ 1 & 0 & 0 & Q \\ d\xi & d\eta & 0 & dv \\ 0 & 0 & d\xi & dw \end{vmatrix} = 0 \tag{40}$$

Substituting equations (37) and (38) into equation (40) results in

$$b_1 du + b_2 dv + b_3 dw + b_4 ds = 0 \tag{41}$$

where

$$b_1 = -A\,(\xi v - \eta w) - \left[a_1 - a_2 \left(\frac{d\xi}{d\eta}\right)_{c\pm}\right] u \tag{42}$$

$$b_2 = -A\eta(\xi v - \eta w) - \left[a_1 - a_2 \left(\frac{d\xi}{d\eta}\right)_{c\pm}\right] \eta u + a_2 \left[(\xi u - w) - (\eta u - v) \left(\frac{d\xi}{d\eta}\right)_{c\pm}\right] \tag{43}$$

$$b_3 = -A\xi(\xi v - \eta w) - \left[a_1 - a_2 \left(\frac{d\xi}{d\eta}\right)_{c\pm}\right] \xi u + \left\{ \frac{a_3 \left[(\xi u - w) - (\eta u - v) \left(\frac{d\xi}{d\eta}\right)_{c\pm}\right]}{\left(\frac{d\xi}{d\eta}\right)_{c\pm}} \right\} \tag{44}$$

$$b_4 = -A \left[a_1 - a_2 \left(\frac{d\xi}{d\eta}\right)_{c\pm}\right] \tag{45}$$

Since the flow properties in the free stream are taken as uniform and there are no rotation producing effects in regions I, II, and III, it is reasonable to assume the flow in the region III is isentropic. Equation (41) then reduces to

$$b_1 du + b_2 dv + b_3 dw = 0 \tag{46}$$

For any streamline

$$\bar{U} \cdot \hat{n} = 0 \tag{47}$$

where $\hat{n}$ is a unit vector normal to the streamline. In the crossflow plane this results in the slope of the streamline being given as

$$\left(\frac{d\xi}{d\eta}\right)_s = \frac{\xi u - w}{\eta u - v} \tag{48}$$

A compatability equation for the streamline may be obtained by multiplying equation (29) by $(\eta u - v)$ and equation (30) by $(\xi u - w)$ and adding them. This results in

$$(\eta u - v)\left(\frac{\partial u}{\partial \eta} + \eta\frac{\partial v}{\partial \eta} + \xi\frac{\partial w}{\partial \eta}\right) + (\xi u - w)\left(\frac{\partial u}{\partial \xi} + \eta\frac{\partial v}{\partial \xi} + \xi\frac{\partial w}{\partial \xi}\right) = 0 \tag{49}$$

Substituting equation (48) and using the definition of a total derivative reduces equation (49) to

$$du + \eta\, dv + \xi\, dw = 0 \tag{50}$$

which is valid only along a streamline.

Line BD - Crossflow Sonic Line

Since the governing equations are parabolic along the sonic line, the term under the radical in equation (39) must be zero at a sonic point. This results in both characteristics having the same slope at a sonic point and the two compatability equations represented by equation (39) becomes

$$\left(\frac{d\xi}{d\eta}\right)_{c_2} = \frac{a_1}{a_2} \tag{51}$$

The loss of one of the compatibility relationships is compensated for by the fact that the crossflow Mach number M_c must be unity at the sonic line. The crossflow Mach number is given by

$$M_c^2 = \frac{2}{\gamma-1}\left\{\frac{\frac{1}{M_\infty^2} + \frac{\gamma-1}{2}\left[1 - \frac{(u+\eta v+\xi w)^2}{1+\eta^2+\xi^2}\right]}{\frac{1}{M_\infty^2} + \frac{\gamma-1}{2}\left[1-u^2-v^2-w^2\right]} - 1\right\} \tag{52}$$

Boundary Conditions

The equations obtained by writing equation (41) for both characteristics and equation (50) for the streamline provide a set of three ordinary differential equations for u, v, and w which, with suitable boundary conditions, may be used to solve for the dimensionless velocity distribution in region III. A set of suitable boundary conditions for this area consists of the dimensionless velocity distribution along line BF2 and the condition that the crossflow velocity is sonic along line BD.

III. Computation Techniques

Region I - Prandtl-Meyer Expansion Fan

Using Newton's method of tangents, equation (20) is solved for θ_{cr}. The slope of individual expansion rays is then obtained from equation (18) for equal increments of θ in the range from θ_∞ to θ_{cr} and used with equation (19) to establish the locus of the expansion rays. The velocity components along each ray are found by solving equations (9) and (15), using the respective values of θ, and substituting the results into equations (10), (11), and (12).

Line BF - Reflection of First Expansion Ray From the Sonic Line

The locus of the reflection of the first expansion ray is found by an iteration technique in which the initial assumption is that the reflection has a vertical slope between the points B and A_1 which are on the successive expansion rays i and i+1 as shown in Fig. 4. The position of point B is known since it is the intersection of ray i and the first reflection. Point A_1 is the intersection of expansion ray i+1 and the first reflection and is determined by equations (23), (5), (18), and (19).

The reflection of the first expansion ray is a characteristic for region III and its slope $\left(\frac{d\xi}{d\eta}\right)_{c+}$ at A_1 is

obtained by substituting ξ_{A_1}, η_{A_1}, and the velocity components for ray (i+1) into equation (39). Using this value of slope a straight line is passed through point A_1. The intersection C of this line and ray i is found. The

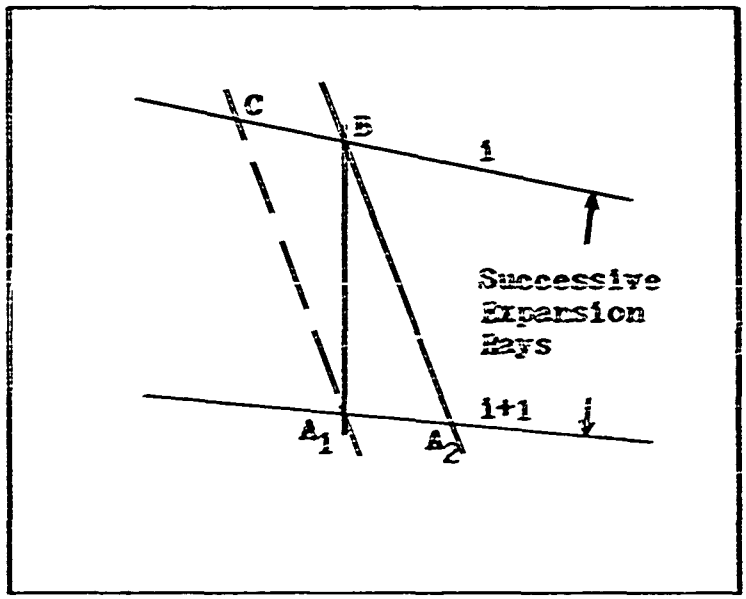

Figure 4. Locating First Reflection

distance between C and B is then determined and, if it is larger than specified limits, the procedure is restarted by assuming the value of $\left(\frac{d\xi}{d\eta}\right)_{c+}$ at A_1 for the slope of the first reflection at point B and determining point A_2 as the new intersection of ray i+1 and the first reflection.

Line BD - Crossflow Sonic Line

A sketch indicating the geometry used in solving for the first point down the sonic line is shown in Fig. 5.

Curve AE is the cone of excitation; lines EC and DE are expansion rays; line ED is a segment of the reflection of the first expansion ray; lines DI and DI' are first family characteristics; and lines EF and EG are streamlines. Although the geometric sketch in Fig. 5 is related to

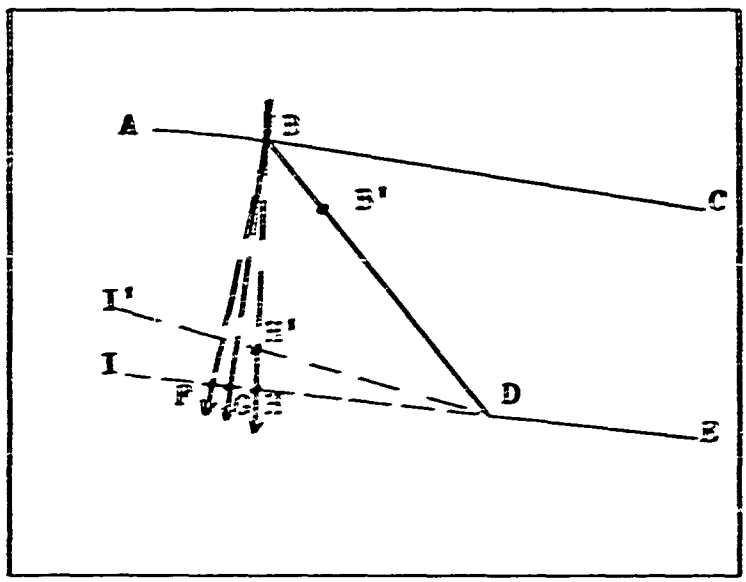

Figure 5. Locating Sonic Point

solution of the first sonic point, the procedure provided below is valid for all sonic points.

The streamline slope based on the properties at E is computed using equation (48) and a line with this slope is passed through E. The slope of the first family characteristic based on the flow conditions at D $\left(\frac{d\xi}{d\eta}\right)_{c+_D}$ is computed from equation (39) and a line with this slope is passed through D to intersect the streamline at F.

The value of $\left(\frac{dy}{dx}\right)_{c^+_D}$ is substituted in the left side of equation (51). The resulting equation is used with equations (46) and (50) to solve for the velocity components at P.

The slope of the streamline at P is then computed from equation (48) and averaged with the slope of the streamline at E. A streamline with this average slope is passed through E to intersect characteristic DI at G. With the value of the slope of line DG substituted into equation (51), equations (46), (50), and (51) are solved for the velocity components at G. The slope of the streamline at G is then computed from equation (48) and averaged with the slope of line EG. A streamline with this averaged slope is passed through E to intersect characteristic DI at H. With the value of the slope of line DH substituted into equation (51), equations (46), (50), and (51) are solved for the velocity components at H. These velocity components and the coordinates of H are then substituted into equation (52) to determine the crossflow Mach number at H.

If the crossflow Mach number is not sufficiently close to unity, a new point H', which is located at a small distance from H and on the streamline EH, is selected. Using the slope of the line DH', the velocity components at H' are determined and the crossflow Mach number computed. This procedure is repeated until a position on the line EH is found where the crossflow Mach number is within ±0.001 of unity.

After a sonic point has been found, the flow conditions along the second family characteristic passing through the sonic point are determined by the procedure described in the following section. However, if the position of any point along this characteristic can not be determined within the specified limits, a new point B' on the line BD is selected as the point through which to pass the initial streamline and the entire sonic point procedure is repeated.

Region III - Field Points

A geometric sketch related to the solution of the flow field in region III is given in Fig. 6. Although the sketch and the procedure outlined below refer to a particular point in the region, the procedure is completely general. The lines labled by I's and II's are first and second family characteristics respectively. Lines BD and B'D' are streamlines.

Using the known conditions at B the slope of the streamline is computed from equation (48) and a line with that slope is passed through B. Using the conditions at C the slope of the first family characteristic is computed and a line with this slope is passed through C to intersect the streamline at D. In this case, as opposed to the sonic line case, equations (41) represent two characteristic compatability relations and these relations are used with equation (50) to solve for the velocity components at D.

The conditions at D are then used to compute the slope

of the second family characteristic $\left(\frac{dy}{dx}\right)_{c+D}$ from equation (39). This slope is averaged with the slope of the second family characteristic at A as computed from equation (39) and a line with the average slope is passed through D to

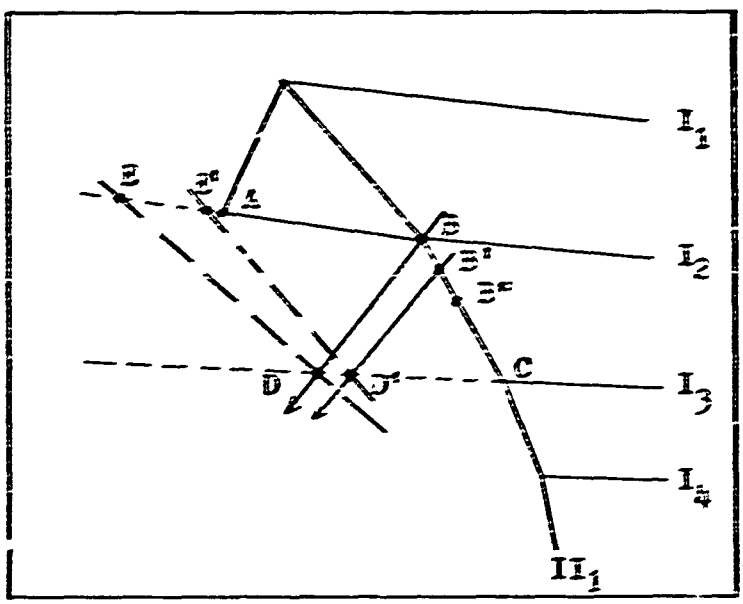

Figure 6. Locating Field Point

intersect line AB at E.

If the distance from E to A is not sufficiently small, a new point B' on BC is selected and the slope of the streamline at B' is computed. A line with this slope is passed through B' to intersect the first family characteristic CD at D'. The velocity components at D' are determined and the slopes of the second family characteristics at D' and A are averaged and the point E' is found in same manner as E. The distance E' to A is determined and, if it

is not within limits, the entire process is repeated with a new point P^*.

IV. Discussion of Results

Numerical solutions were obtained for the following sets of input data with 100 expansion rays in region I:

1) $M_\infty = 2.96$, $\alpha = 14.2^\circ$, $\chi = 45.0^\circ$;

2) $M_\infty = 4.0$, $\alpha = 5.0^\circ$, $\chi = 60.0^\circ$;

3) $M_\infty = 3.0$, $\alpha = 12.0^\circ$, $\chi = 45.0^\circ$.

Data Set 1

This data set was used by Bannink, Nebbeling, and Reyn as the conditions for an experimental investigation of the flow field. A plot of the characteristic network in regions I and III as computed by the procedures outlined in Chapter III is given in Fig. 7. Only every twentieth ray was plotted for clarity reasons. Experimental data taken from Bannink, Nebbeling, and Reyn are included in this figure. This data indicates the location of the internal shock wave, as determined by pitot pressure measurements, in the cross-flow plane at various distances from the apex.

As noted by Bannink, Nebbeling, and Reyn the first Prandtl-Meyer expansion ray lies just downstream of the experimental location of a leading edge shock and the final expansion ray is very near the experimental location of the reattachment shock.

The crossflow sonic line is very nearly straight in the

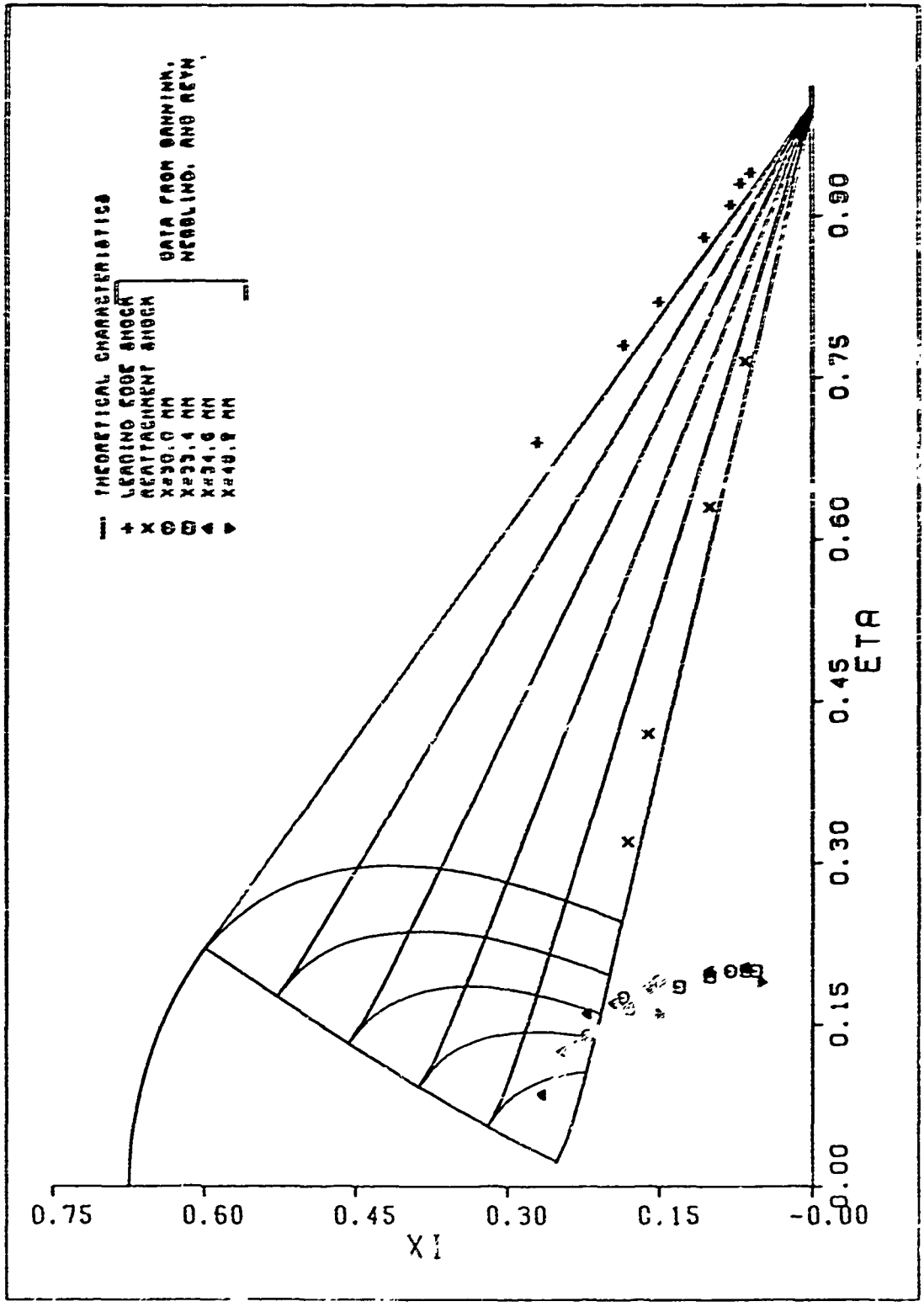

Figure 7. Characteristic Network for N_{∞}=2.96, α=14.2°, χ=45.0°

area of the intersection of the Mach cone and the first expansion ray. However, the amount of curvature of the sonic line increases in the region near the plane of symmetry. It was expected that the sonic line would terminate at the last point on the experimental shock curve. As indicated in Fig. 7, this is not the case. Two possible causes of this difference are the inviscid flow assumption and error in the numerical technique.

It is noted that the first family characteristics curve upward as region III is traversed in the inboard direction. This is in opposition to the qualitative sketch of the crossflow plane proposed by Bannink, Nebbeling, and Reyn and supports the views of Hays and Probstein (Ref 9:532).

The computed static and pitot pressure ratios, P/P_∞ and P_p/P_{p_∞} respectively, at $\xi = 0.266$ are given in Fig. 8. This figure also includes experimental data for P_p/P_{p_∞} taken from Bannink, Nebbeling, and Reyn. The calculated and experimental pressure ratios agree well up to the point just prior to the shock wave where the experimental data indicates recompression begins.

Figure 9 is a plot of the slope of the streamline traces in the crossflow plane. The point for which the streamline slope is computed is at the center of each trace. It is noted that the streamline traces along the sonic line are nearly parallel to the sonic line. However, computations show that the slope of the sonic line is slightly greater than the slope of the streamline traces.

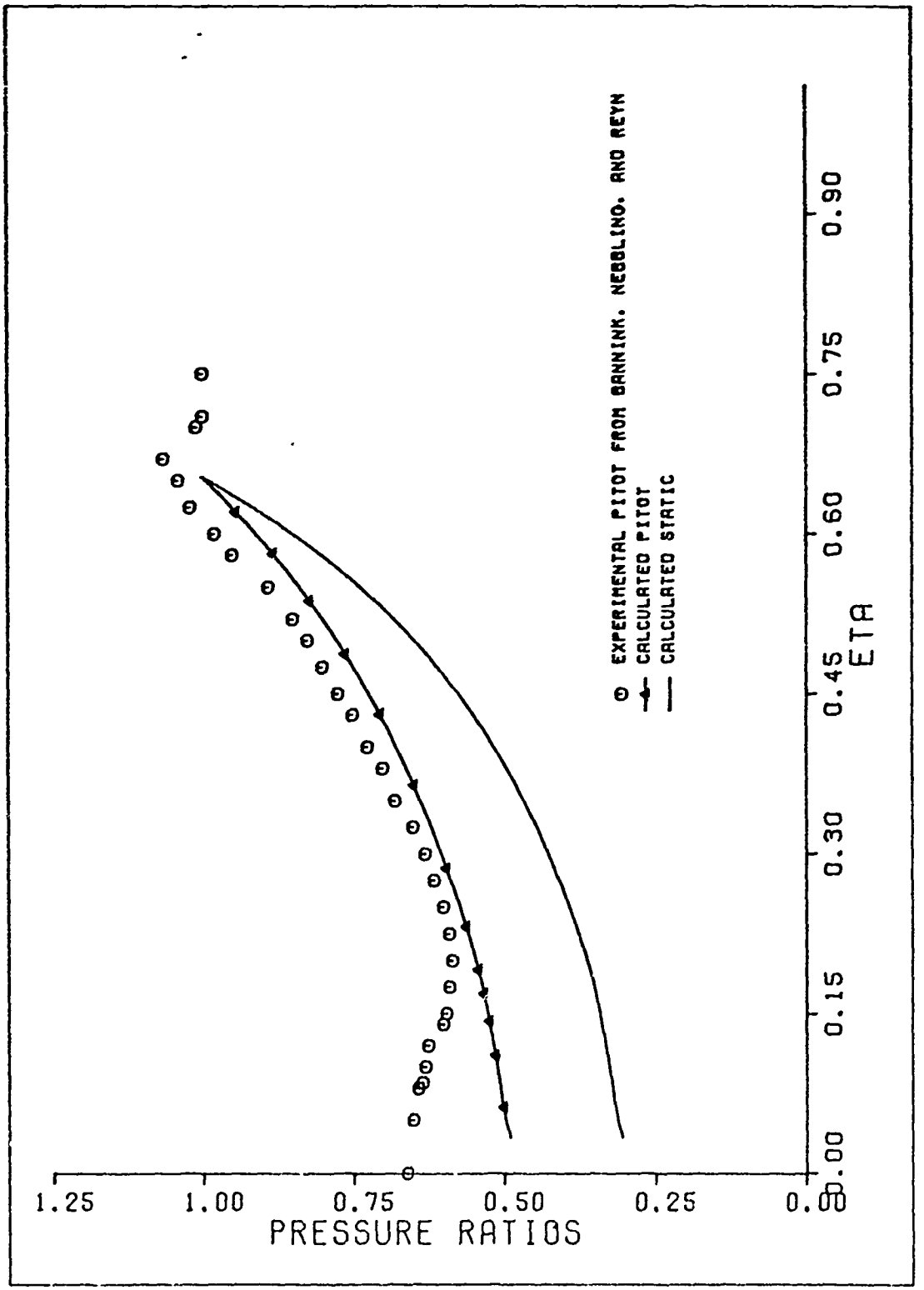

Figure 8. Pressure Ratios at $\xi=0.266$ for $M_\infty=2.96$ $\alpha=14.2^\circ$, $\chi=45.0^\circ$

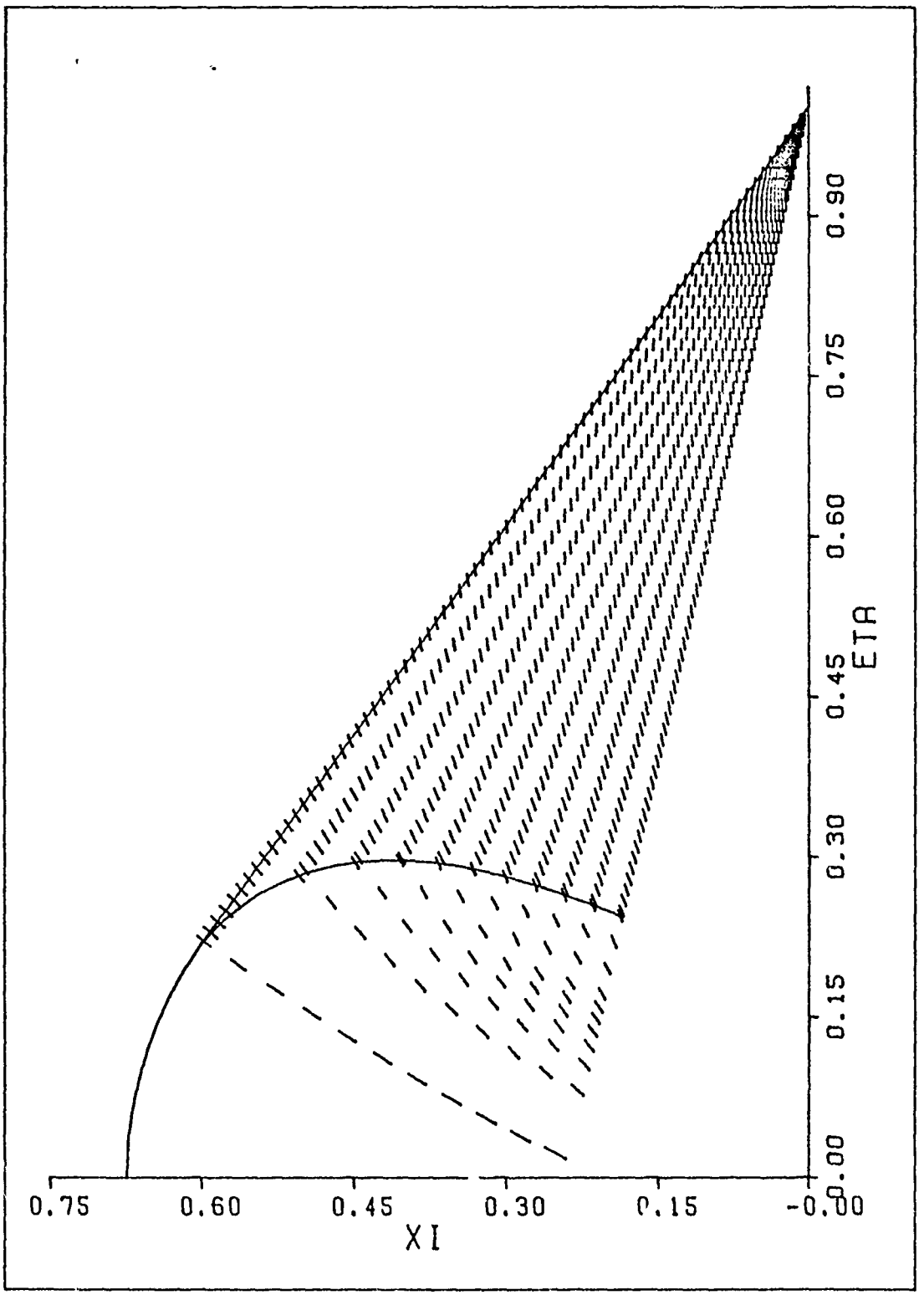

Figure 9. Streamlines for M_∞=2.96, α=14.2°, χ=45.0°

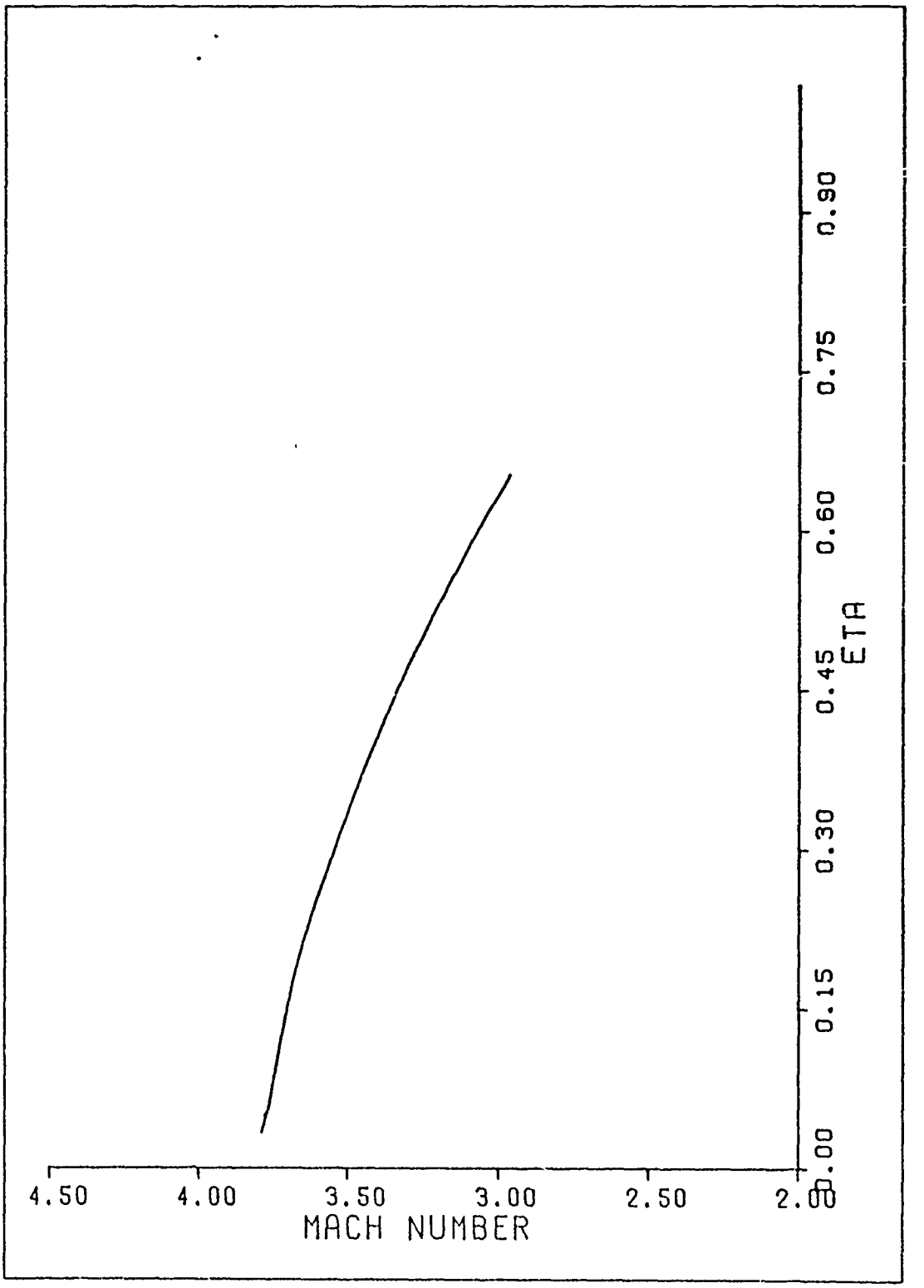

Figure 10. Mach Number for M_∞=2.36, α=14.2°, x=45.0°

The total Mach number distribution at ξ = 0.266 is given in Fig. 10. The Mach number increases uniformly from a free stream value of 2.96 to a value of 3.79 at the crossflow sonic line.

Data Set 2

The characteristic network in region I and III is plotted in Fig. 11 for this data set. This data set is also one of the sets of conditions for which Babayev presented a solution. The solution of the flow field in region I as given here and that presented by Babayev are in complete agreement. However, there is considerable difference between the two solutions for region III. The crossflow sonic line given by Babayev is also plotted in Fig. 11. The difference in the location of this line is a result of the planar shock assumption. Experimental data is not available for this data set but, in an analogous study, Bannink, Nebbeling, and Reyn did not confirm the existence of a planar shock wave.

The computed static and pitot pressure ratios at ξ = 0.266 for this input data are given in Fig. 12. Figure 13 is a plot of the streamline traces and Fig. 14 gives the Mach number distribution at ξ = 0.266.

The program was run with this set of input data and with ten Prandtl-Meyer expansion rays in region I. The most significant difference was that the terminal position of the sonic line was shifted slightly inboard and lower.

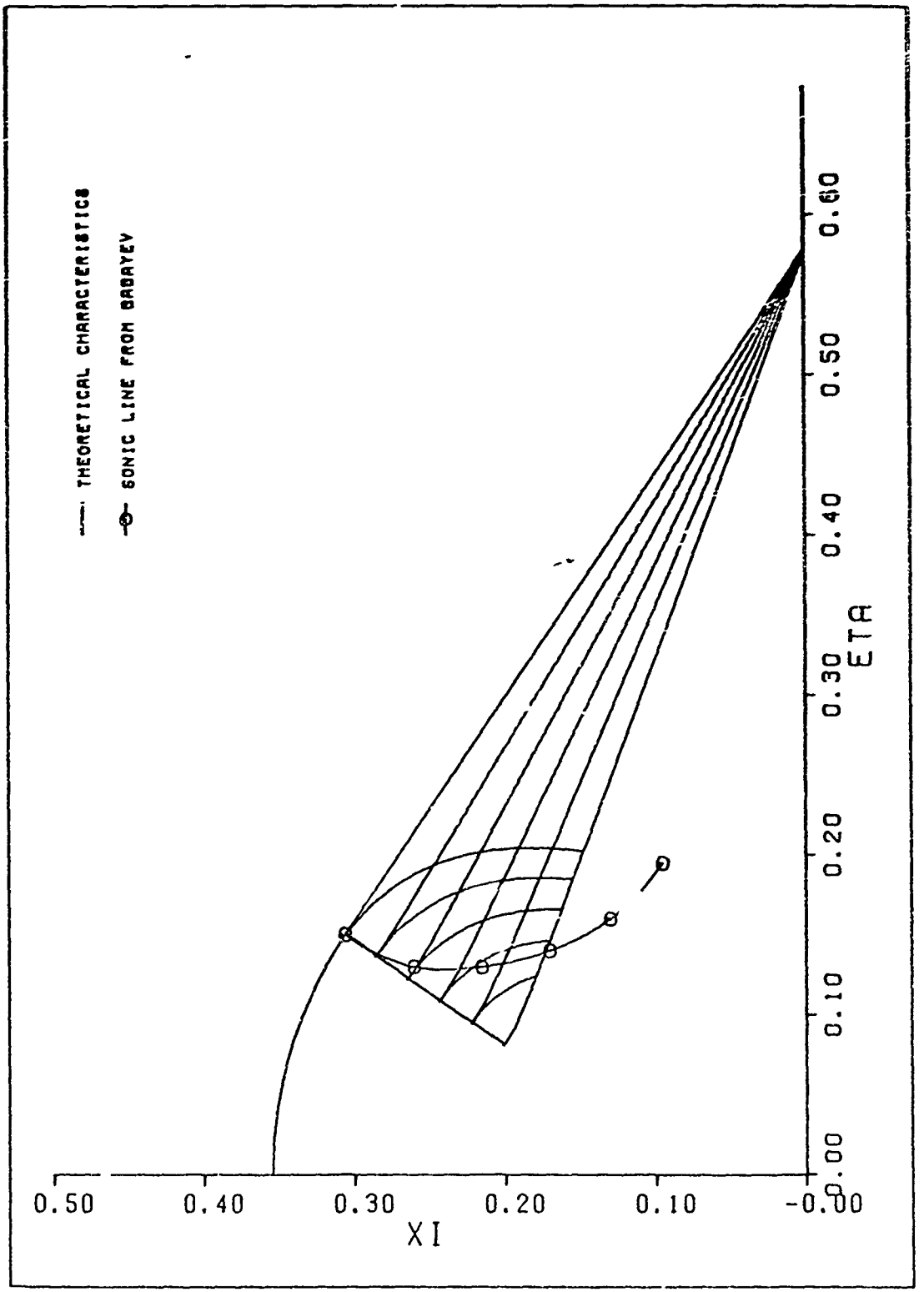

Figure 11. Characteristic Network for M_∞=4.0, α= 5.0°, χ=60.0°

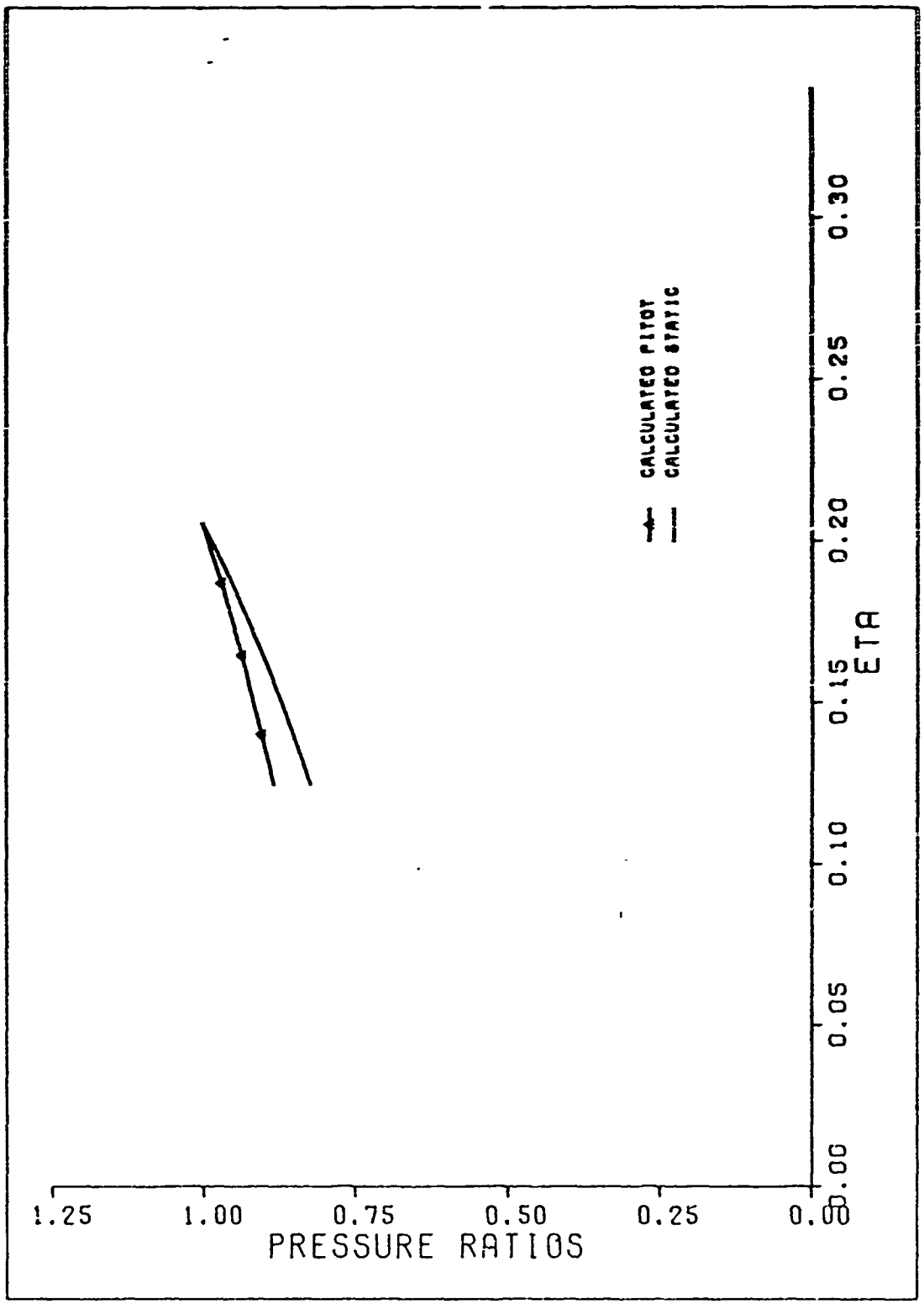

Figure 12. Pressure Ratios at ξ =0.266 for M_∞=4.0, α=5.0, χ=60.0°

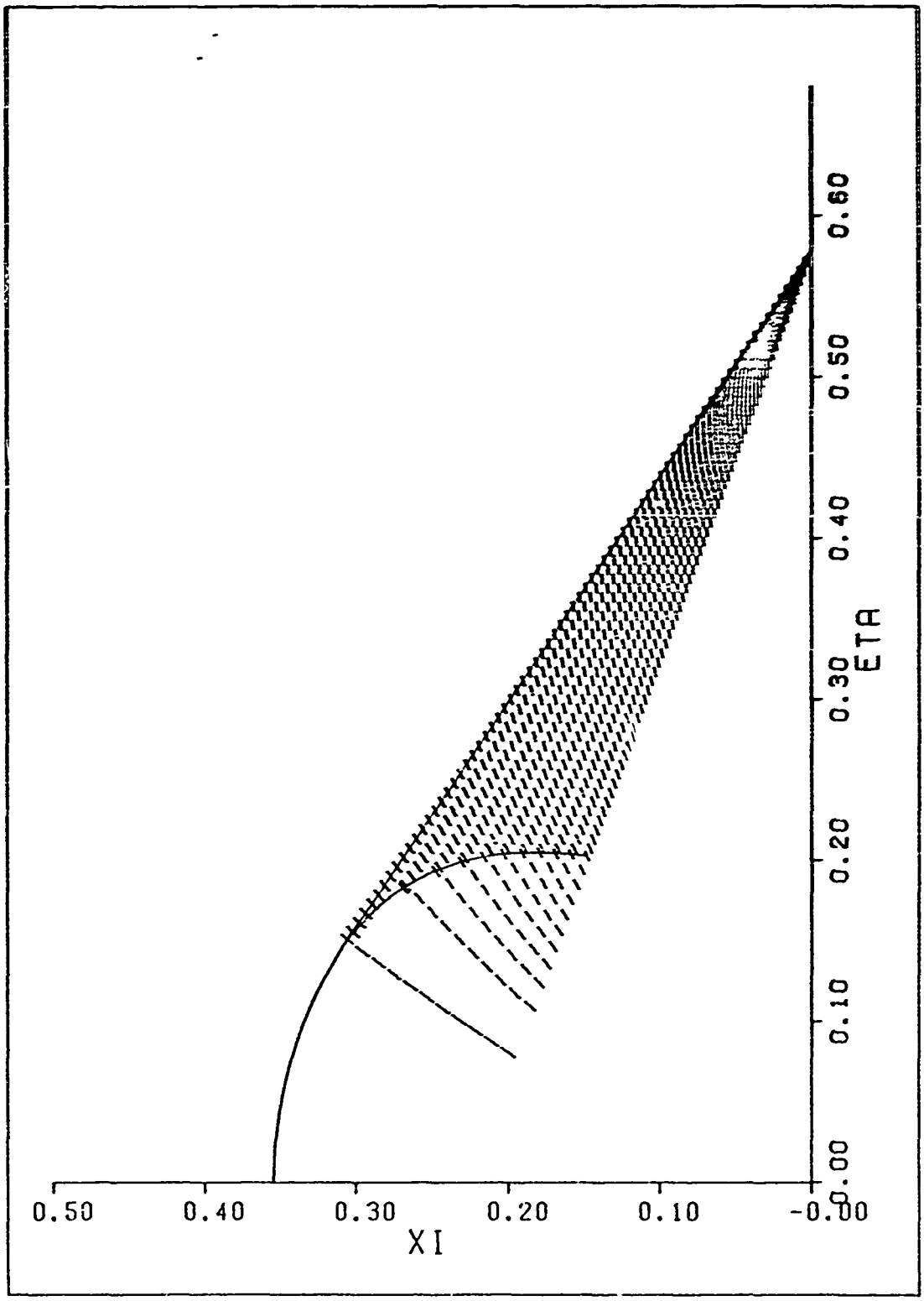

Figure 13. Streamlines for M_∞=4.0, α=5.0°, χ=60.0°

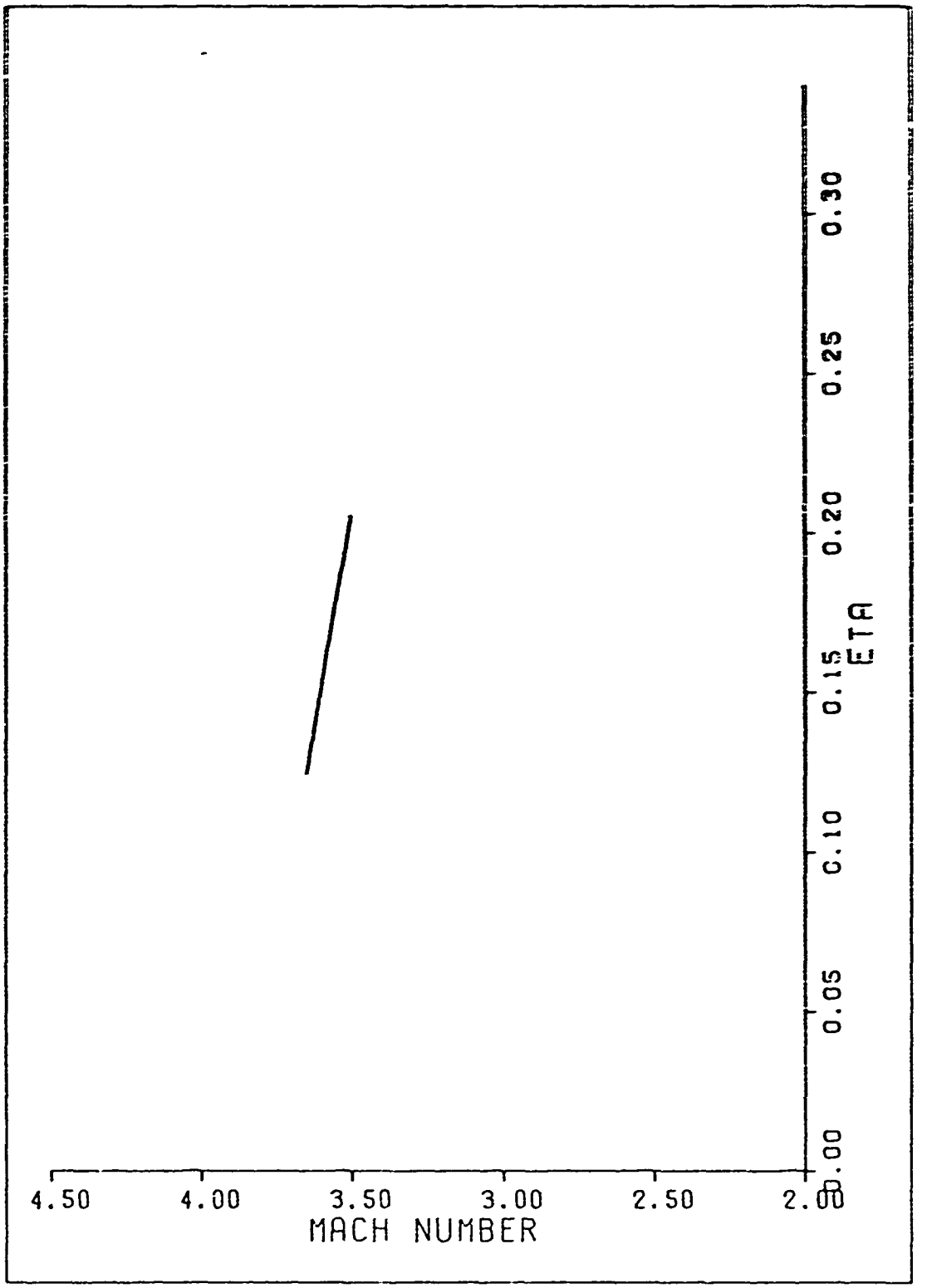

Figure 14. Mach Number at ξ =0.266 for M_∞=4.0, α=5.0°, χ=60.0°

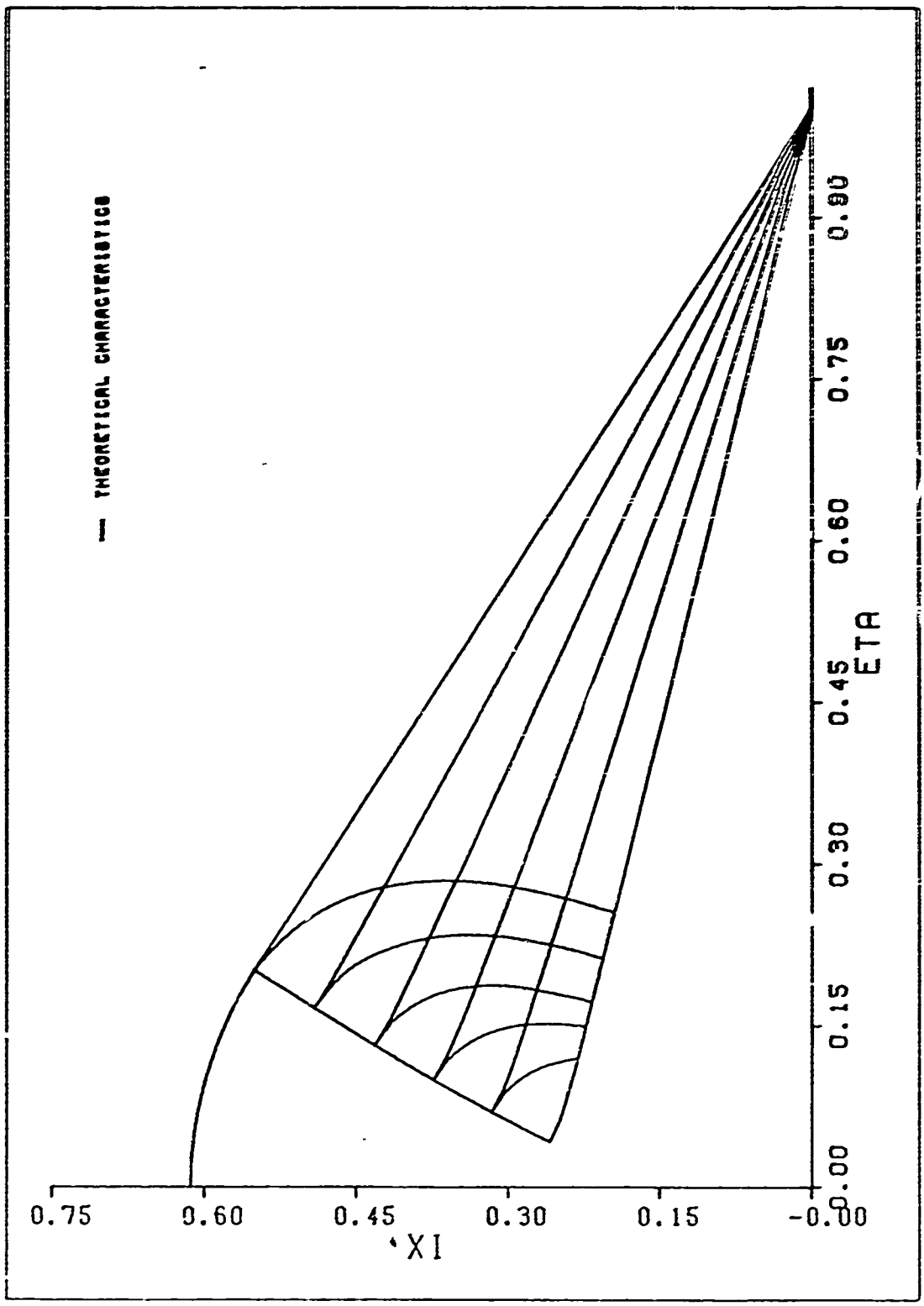

Figure 15. Characteristic Network for M_∞=3.0, α=12.0, γ=1.4

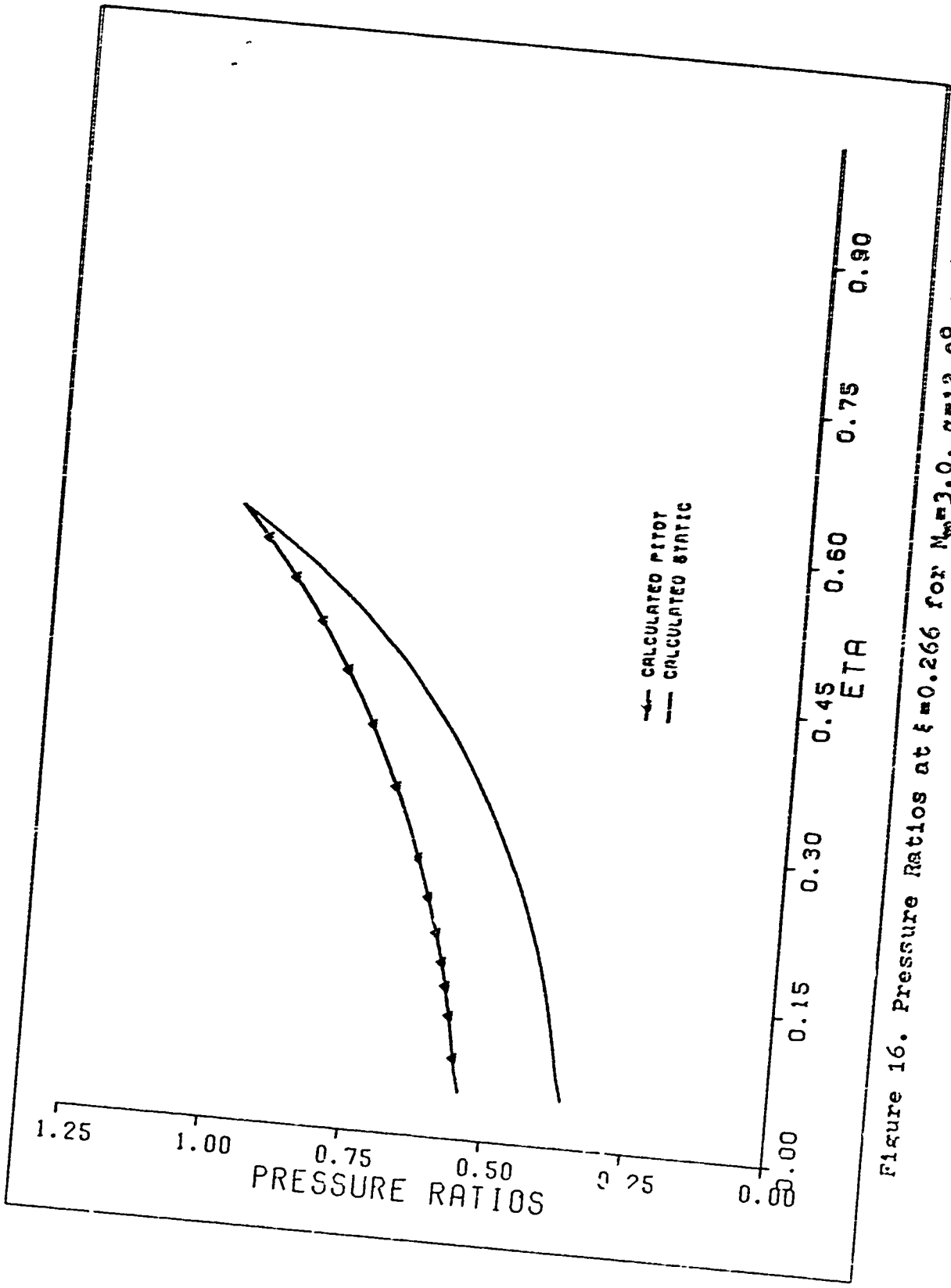

Figure 16. Pressure Ratios at ξ=0.266 for M_∞=3.0, α=12.00°, χ=45.00°

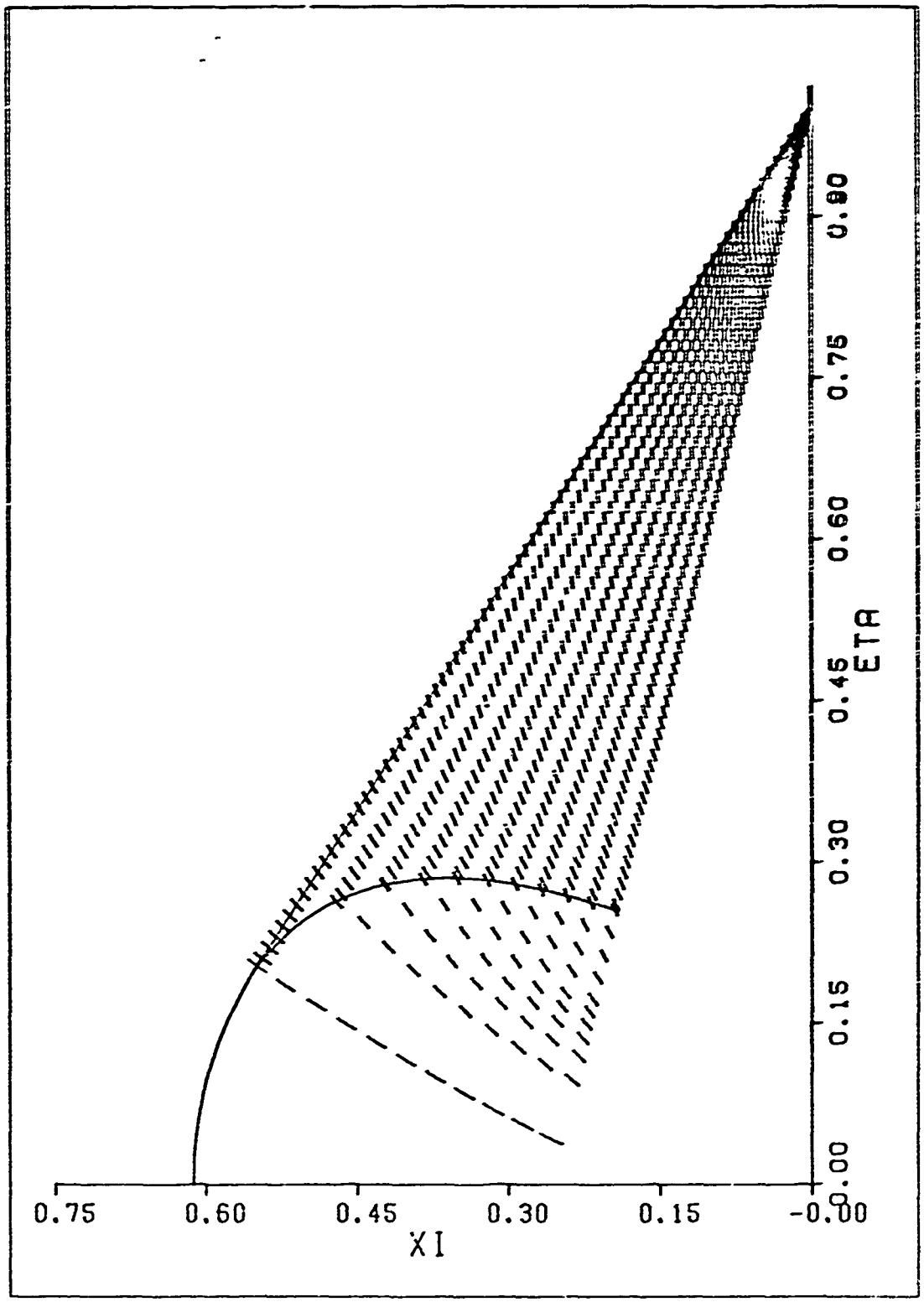

Figure 17. Streamlines for M_∞=3.0, α=12.0, γ=45.0°

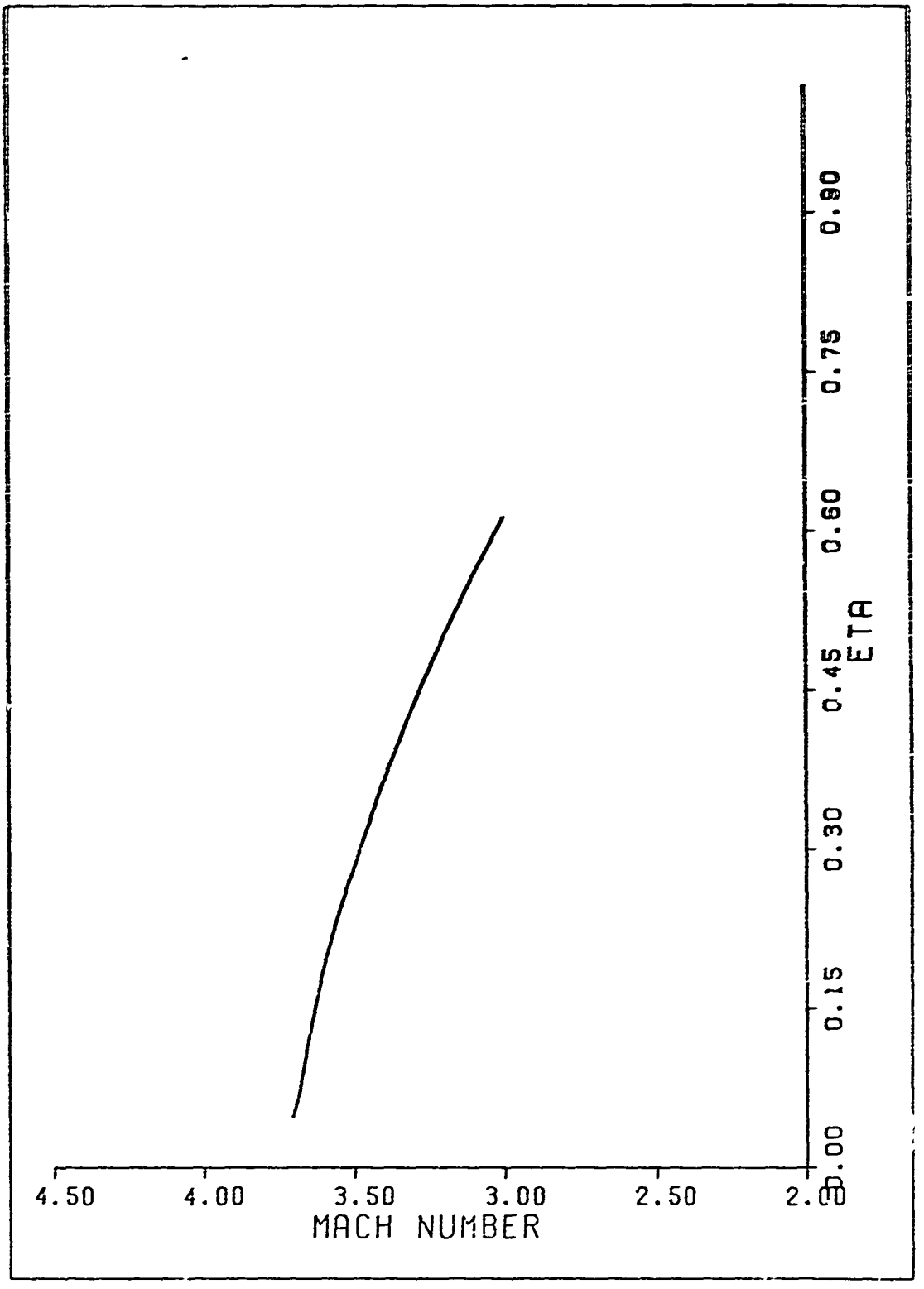

Figure 18. Mach Number at ξ=0.266 for M_∞=3.0, α=12.0°, χ=45.0°

Data Set 3

The characteristic network for this data set is given in Fig. 15. Figure 16 is a plot of the static and pitot pressure ratios at $\xi = 0.266$ and Figs. 17 and 18 are plots of the streamline traces and the Mach number distribution at $\xi = 0.266$, respectively. This data set was used by Maslen who assumed that no shock existed in the flow field.

Additional Cases

An attempt was made to obtain solutions for $M_\infty = 6.0$, $\alpha = 7.0^\circ$ and $\chi = 60.0^\circ$ with 100 Prandtl-Meyer expansion rays and for $M_\infty = 2.96$, $\alpha = 14.2^\circ$ and $\chi = 45.0^\circ$ (Data set 1) with ten Prandtl-Meyer expansion rays. The procedure used to determine the location of reflection of the first expansion ray diverged and no results were obtained.

V. Conclusions and Recommendations

Conclusions

The following conclusions are made from this study.

1. It is possible to obtain a solution for the flow field in the pseudo-elliptic region by use of the method of characteristics.

2. The predicted pressure ratios in the pseudo-elliptic region were in reasonable agreement with the available experimental data.

3. Numerical solutions were not obtained for two sets of input conditions as a result of a deficiency in the procedure used to locate the reflection of the first expansion ray.

4. The accuracy of the terminal position of the cross-flow sonic line was improved with the increase in the number of expansion rays.

5. The slope of the streamlines along the sonic line is very near to the slope of the sonic line. This indicates that most of the fluid in the pseudo-elliptic region exits this region through the curved shock wave. Therefore, a significant portion of the flow field governed by elliptic equations is rotational.

Recommendations

The following items are recommended as areas for further study.

1. An attempt should be made to improve the accuracy of the solution by modifying the procedure used to locate the sonic points.

2. A study should be undertaken to improve the technique for locating the reflection of the first expansion ray. This would broaden the usefulness of the procedure and allow for further characterization of the flow field.

3. An experimental investigation of the flow field similar to that conducted by Bannink, Nebbeling, and Reyn but for a wide range of free stream Mach numbers, angles of attack, and sweep angles would provide additional data for further verification of analytical solutions.

4. A study of the elliptic regions should be conducted using the procedure developed in this study to determine the boundary conditions.

5. An analytical study should be undertaken to include the effects of viscosity and a curved wing.

Bibliography

1. Babayev, D. A. "Numerical Solution of the Problem of Flow Around the Upper Surface of a Triangular Wing By a Supersonic Stream." U.S.S.R. Comp. Math. Math. Physics, 2:296-309 (1962).

2. Bannink, W. J., C. Nebbeling, and J. W. Reyn. Investigation of the Flow Field on the Expansion Side of a Delta Wing with Supersonic Leading Edges. Report VTH-128. Delft, The Netherlands: Technological University Delft, August 1965.

3. Beeman, E. R. and S. A. Powers. A Method For Determining the Complete Flow Field Around Conical Wings at Supersonic/Hypersonic Speeds. AIAA Paper 69-646. New York: American Institute of Aeronautics and Astronautics, June 1969.

4. Bulakh, B. M. and J. W. Reyn. "Remarks on the Problem of the Delta-Shaped Wing." J. Appl. Math. Mech., 31: 207-210 (1967).

5. Busemann, A. "Drüke auf kegelförmige Spitzen bei Bewegung mit Uberschallgeschwindigkeit." Z. augew. Math. Mech., 9: 496-498 (1929).

6. Chaing, C. W. and R. D. Wagner, Jr. Analysis of Supersonic Conical Flows. NASA TN D-5884. Washington: National Aeronautics and Space Administration, 1970.

7. Cross, E. J. and W. L. Hankey. Investigation of the Leeward Side of a Delta Wing at Hypersonic Speeds. AIAA Paper 68-675. New York: American Institute of Aeronautics and Astronautics, June 1968.

8. Fowell, L. R. "Exact and Approximate Solutions for the Supersonic Delta Wing." J. of the Aeronautical Sciences, 23: 709-720, 770 (August 1956).

9. Hayes, W. D. and R. F. Probstein. Hypersonic Flow Theory - Volume I (second edition). New York: Academic Press Inc., 1966.

10. Kitowski, J. V. Unpublished papers.

11. Kutler, P. and H. Lomax. A Systematic Development of the Supersonic Flow Fields Over and Behind Wings and Wing-Body Configurations Using a Shock-Capturing Finite-Difference Approach. AIAA Paper 71-99. New York: American Institute of Aeronautics and Astronautics; January, 1971.

12. Liepmann, H. W. and A. Roshko. Elements of Gasdynamics. New York: John Wiley and Sons, Inc., 1957.

13. Maslen, S. H. Supersonic Conical Flows. NACA TN 2651. Washington: National Advisory Committee for Aeronautics, March 1962.

Appendix A

Development of Velocity Equation

The development of the velocity equations as given here was suggested by Kitowski (Ref 10).

The total velocity vector at any point in region I can be separated into the components normal and parallel to the leading edge of the wing. Resolving these components into components along the XYZ coordinates and dividing by V_∞ results in

$$u = \frac{V_n}{V_\infty} \cos(\alpha_1 - \delta) \cos x + \frac{V_t}{V_\infty} \sin x \qquad \text{(A-1)}$$

$$v = -\frac{V_n}{V_\infty} \cos(\alpha_1 - \delta) \sin x + \frac{V_t}{V_\infty} \cos x \qquad \text{(A-2)}$$

$$w = \frac{V_n}{V_\infty} \sin(\alpha_1 - \delta) \qquad \text{(A-3)}$$

where α_1 is the angle between the surface of the wing and the component of the free stream velocity normal to the leading edge and δ is the angle through which the normal component of the free stream is deflected; α_1 and δ are given by equations (13) and (9) respectively.

The component of velocity parallel to the leading edge is unaffected by the expansion process and is given by

$$V_t = V_\infty \cos \beta \tag{A-4}$$

where β is the angle between the leading edge of the wing and the free stream velocity vector and is given by equation (14).

The component of velocity normal to the leading edge is

$$V_n = M_n c \tag{A-5}$$

Using isentropic flow relationships this becomes

$$V_n = M_n \, c_\infty \left[\frac{1+\frac{\gamma-1}{2} M_{n_\infty}^2}{1+\frac{\gamma-1}{2} M_n^2} \right]^{\frac{1}{2}} \tag{A-6}$$

and, since $M_{n_\infty} = M_\infty \sin \beta$

$$V_n = M_n \, c_\infty \left[\frac{1+\frac{\gamma-1}{2} M_\infty^2 - \frac{\gamma-1}{2} M_\infty^2 \cos^2 \beta}{1+\frac{\gamma-1}{2} M_n^2} \right] \tag{A-7}$$

Thus, $$\frac{V_n}{V_\infty} = \frac{M_n}{M_\infty} \left[\frac{1 + \frac{\gamma-1}{2} M_\infty^2 - \frac{\gamma-1}{2} M_\infty^2 \cos^2 \beta}{1 + \frac{\gamma-1}{2} M_n^2} \right]^{\frac{1}{2}} \tag{A-8}$$

$$\text{or} \qquad \frac{V_n}{V_\infty} = \left[\frac{\frac{2}{\gamma+1}\frac{1}{M_\infty^2}\left(1 + \frac{\gamma-1}{2} M_\infty^2\right) - \frac{\gamma-1}{\gamma+1}\cos^2\beta}{\frac{2}{\gamma+1}\frac{1}{M_\infty^2}\left(1 + \frac{\gamma-1}{2} M_n^2\right)} \right]^{\frac{1}{2}} \tag{A-9}$$

From equation (7), M_n^2 is given by

$$M_n^2 = 1 + \frac{\gamma+1}{\gamma-1} \tan^2 \sqrt{\frac{\gamma-1}{\gamma+1}}\,\theta \tag{A-10}$$

and equation (A-9) becomes

$$\frac{V_n}{V_\infty} = \left\{ \frac{\frac{2}{\gamma+1}\frac{1}{M_\infty^2}\left(1 + \frac{\gamma-1}{2} M_\infty^2\right) - \frac{\gamma-1}{\gamma+1}\cos^2\beta}{\left(\frac{\gamma-1}{\gamma+1}\right)\left[\frac{(\gamma+1) + (\gamma+1)\tan^2\sqrt{\frac{\gamma-1}{\gamma+1}}\,\theta}{(\gamma-1) + (\gamma+1)\tan^2\sqrt{\frac{\gamma-1}{\gamma+1}}\,\theta}\right]} \right\}^{\frac{1}{2}} \tag{A-11}$$

which reduces to

$$\frac{V_n}{V_\infty} = \left\{ \left[\frac{2}{(\gamma+1) M_\infty^2} + \left(\frac{\gamma-1}{\gamma+1}\right)\left(1 - \cos^2\beta\right) \right] \left[1 + \frac{2}{\gamma-1} \sin^2 \sqrt{\frac{\gamma-1}{\gamma+1}}\,\theta \right] \right\}^{\frac{1}{2}} \tag{A-12}$$

Substituting equations (A-4) and (A-12) into equations (A-1), (A-2), and (A-3) and then using b as defined by equation (15) results in equations (10), (11), and (12) respectively.

VITA

Robert Gene Christophel was born in Glendale, Ohio on May 21, 1939. He graduated from high school in 1957 and enlisted in the U.S. Air Force in 1958. His primary duty as an enlisted member of the Air Force was as a weather observer. From 1960 to 1965, while being assigned to various Air Force stations in the United States and overseas, he intermittently enrolled in night classes offered by the University of Maryland, Southern Florida College, and the University of Omaha. In 1968 he was accepted into the Airmen's Educationing and Commissioning Program and assigned to Oklahoma State University from which he was granted a Bachelors of Science degree in Aerospace Engineering in 1970. He was commissioned as a 2Lt in the U.S. Air Force at Lackland AFB, Texas later tnat year and was then assigned to the Air Force Institute of Technology at Wright-Patterson AFB, Ohio.

Permanent address: 6526 State Road
Somerville, Ohio

This thesis was typed by Mrs. Anne E. Posner